Appl Phys A (2012) 109:441–448
DOI 10.1007/s00339-012-7048-6

Applied Physics A
Materials Science & Processing

Sapphire surface patterning using femtosecond laser micromachining

Cho-Wei Chang · Chien-Yu Chen · Tien-Li Chang · Chia-Jen Ting · Chien-Ping Wang · Chang-Pin Chou

Received: 11 February 2012 / Accepted: 2 July 2012 / Published online: 18 July 2012
© Springer-Verlag 2012

Abstract This study presents an alternative method for micron-resolution patterning of a sapphire surface utilizing the characteristic of an ultra-short pulse (10^{-15} s) from ytterbium (Yb) femtosecond laser (FS-laser) irradiation. Conventional processes often involve several steps, such as wet chemical or dry etching, for surface structuring of sapphire. In this study, two-dimensional array patterns on the sapphire surface with an area of 5×5 mm^2 and a depth of 1.2 ± 0.1 μm can be directly and easily fabricated by a single step of the FS-laser process, which involves 350-fs laser pulses with a wavelength of 517 nm at a repetition rate of 100 kHz. The measured ablation depths on the sapphire surface display that the proposed process can be under well-controlled conditions. Based on the design changes for being quickly implemented in the micromachining process, a FS laser can be a promising and competitive tool for patterning sapphire with an acceptable quality for industrial usage.

C.-W. Chang · C.-P. Chou
Department of Mechanical Engineering, National Chiao Tung University, Hsinchu 300, Taiwan, R.O.C.

C.-Y. Chen
Institute of Nanotechnology and Microsystems Engineering, Department of Materials Science and Engineering, National Cheng Kung University, Tainan 701, Taiwan, R.O.C.

T.-L. Chang (✉)
Department of Mechatronic Technology, National Taiwan Normal University, 162, Sec. 1, Ho-Ping E. Road, Taipei 106, Taiwan, R.O.C.
e-mail: tlchang@ntnu.edu.tw
Fax: +886-2-23583074

C.-J. Ting
Mechanical and Systems Research Laboratories, Industrial Technology Research Institute, Hsinchu 310, Taiwan, R.O.C.

C.-P. Wang
Electronics and Optoelectronics Research Laboratories, Industrial Technology Research Institute, Hsinchu 310, Taiwan, R.O.C.

1 Introduction

Sapphire (α-Al_2O_3) single crystal is widely used in optoelectronic and microelectronic applications such as blue-emitting diodes, high-power laser optics, laser diode devices, visible–infrared windows, substrates for semiconductor devices and high-pressure components because of its excellent mechanical, electrical and optical properties [1]. However, it is difficult to apply machine tools or chemical machining methods to sapphire because of its high hardness, brittleness and chemical stability [2–4]. In addition, the conventional methods usually create an excessive heat-affected zone (HAZ) that poses limitations for the development of advanced devices [5, 6]. In recent years, considerable efforts have been devoted to using ultra-short laser pulses for micromachining [7].

In general, ultra-short laser pulses (<10 ps) with femtosecond (FS) or picosecond pulse duration can fully ionize almost any solid material with greatly reduced recast, microcracks and HAZ. Hence, an ultra-short laser emerges as a promising tool for micromachining all types of materials [8–10]. Different from that of conventional lasers, the energy flux of an ultra-short laser at the focus is very high ($>10^{11}$ W/cm^2) when its laser beam is converged to a small focal spot [11], thus inducing optical breakdown and removing the material via plasma-mediated ablation. The generation and absorption of substantial plasma can cause the ablation of materials which are normally difficult to ablate using conventional lasers, such as transparent or low-absorption materials [12, 13]. In addition, the short pulse width of an ultra-short laser offers a key advantage over a long-pulse

laser in depositing energy into a material within a short time before any thermal diffusion can occur [14, 15]. Due to the very short time scales involved in the ablation with ultra-short laser pulses, the ablation process can be considered as a direct solid–vapor (or solid–plasma) transition. The physical phenomena associated with the interaction of an ultra-short laser pulse at the femtosecond time scale have been reported by Rethfeld et al. [16]. Their work indicates that ablation occurs roughly on a nanosecond time scale for the relevant process. This reference also provides a clear example for calculating the electron and lattice temperatures with time in gold from the two-temperature model [17].

In recent years, the use of ultra-short laser pulses as an important fabrication process has been studied. Gertus et al. [18] used FS-laser pulses to pattern the surface and volume of dielectric materials such as borosilicate glass. Compared with long-pulse laser ablation, the advantage of ultra-short laser ablation lies in its ability to produce very high peak-power intensity and to deliver energy into a material before thermal diffusion occurs. Hence, dielectric materials can be easily patterned with no cracks formed by the ultra-short laser pulses. Aguilar et al. [19] demonstrated that ultra-short laser pulses can be an excellent tool for micropatterning biodegradable transparent polymers. Moreover, it can be seen that the HAZ of the laser around the machined feature was minimized. Hayden and Dalton [20] presented an alternative method for creating microelectrodes for neuron stimulation using a FS-laser process, which was a single patterning step without having to re-manufacture a photolithographic mask. Wiesner and Ihlemann [21] employed F_2 lasers, which are ultra-short lasers, to fabricate various micro-optical elements, like fiber tip lenses, gratings and diffractive optical elements. Though the material sapphire has been precisely fabricated by F_2 laser ablation at 157 nm, its process control is still in need of a suitable mask projection. With the aim of achieving sapphire surface patterning with a mask-less process, the study of micromachining with a process of FS-laser direct writing is essential.

This study uses FS-laser pulses for patterning the surface of sapphire. Few studies have examined the application of FS-laser irradiation to patterning a sapphire surface. The relationship between the surface of sapphire patterning and processing parameters including energy fluence and scanning speed of the laser is experimentally investigated. Finally, machining of two-dimensional square arrays of sapphire is performed to illustrate that FS-laser pulses could be easily and directly employed to fabricate a sapphire surface.

2 Experimental details

In this experiment, the surface structuring of sapphire with the FS-laser direct writing technique is presented in Fig. 1. This FS-laser system is an all-in-one femtosecond regenerative amplifier system (UC-1035-2000; High Q Laser Production GmbH) with an ytterbium (Yb) laser as the irradiation source. The center wavelength of the FS laser is 1035 nm and a system with frequency multiplication is installed. However, the doubled frequency of a laser wavelength is used at 517 nm when patterning the surface structures of sapphire. The laser system has a maximum output power of about 2.0 W. The repetition rate and pulse width (FWHM) of the FS-laser system are 100 kHz and 350 fs, respectively. The beam profile from this regenerative amplifier system is of approximate Gaussian distribution. In addition, the system includes a correlation filter lens group. The optical lens group is composed of half-wave plates ($1/2\lambda$), polarizing beam splitter (PBS) and iris, which are adopted to attenuate the energy of the Gaussian laser beam. Then, the transmitted laser beam passing through a dichroic mirror is monitored by a charge-coupled-device (CCD) laser focusing system during the entire patterning process. Here, the incident laser beam is irradiated onto the sapphire sample through an objective lens (20×, 0.4 NA, Olympus Inc.). Ultimately, this device can perform precise focusing and processing on sample surfaces by moving a high-precision XY stage (ABL1500; Aerotech Inc.). The CCD focus system is employed to display the real-time pattern process on the linked monitor. All experiments are measured at an atmospheric pressure of 101.325 kPa and room temperature of 25 °C. The sample is then subjected to an ultrasonic bath for 30 min in acetone solution until all debris on the surface of the microstructure device is removed. The surface structuring of sapphire is measured by an optical microscope (OM), an alpha-step profilometer (α-step), a three-dimensional laser confocal microscope and a scanning electron microscope (SEM).

3 Results and discussion

To determine the surface structuring of sapphire, the FS-laser intensity distribution in the focus area has to be carefully controlled. The intensity distribution is measured by imaging the corresponding position in the focus onto the CCD system with an objective lens. The measured FS-laser intensity distribution in the focus of the objective lens is displayed in Fig. 2a. For a Gaussian spatial beam profile, the maximum energy fluence of laser (peak fluence) in terms of its pulse energy can be written as [22]

$$F_0 = 2E_\mathrm{p}/\pi\omega_0^2, \tag{1}$$

where F_0 is the maximum energy fluence of the laser, E_p is the threshold pulse energy and ω_0 is the focused beam

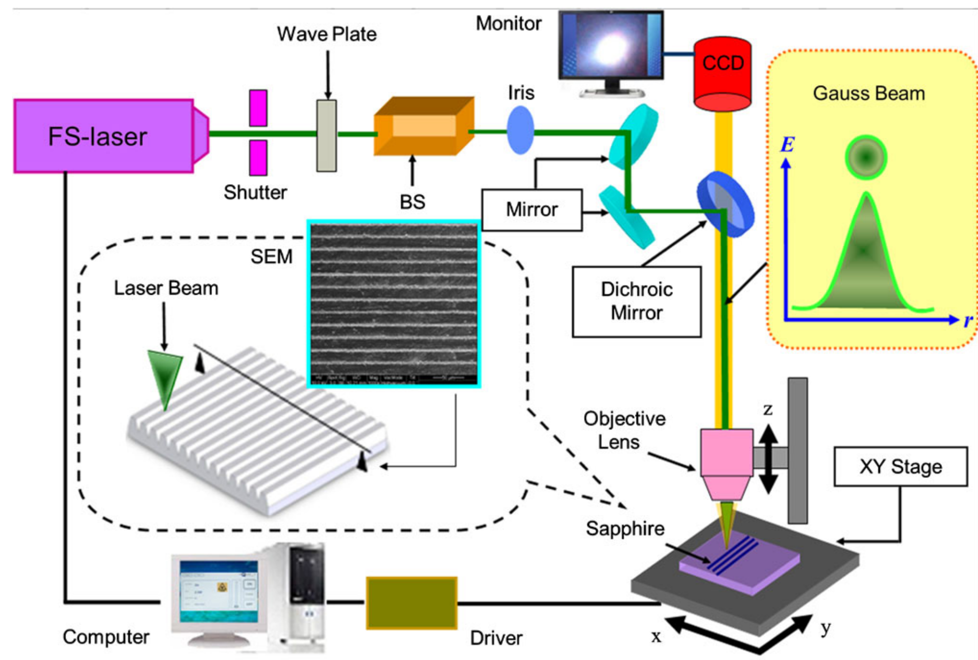

Fig. 1 Schematic of experimental setup for surface structuring of sapphire with FS-laser irradiation. The system delivers laser pulses at 517 nm with a pulse width of 350 fs (FWHM) and a repetition rate of 100 kHz. Mounted on a computer that controls the positioning, the sample is moved in small steps along x, y and z axes

radius. If the maximum energy fluence F_0 exceeds the ablation threshold fluence (F_{th}), the diameter of laser ablation (D) in terms of pulse energy can be expressed as [22, 23]

$$D = \omega_0 \sqrt{2 \ln\left(\frac{F_0}{F_{th}}\right)}, \tag{2}$$

where $D = 2r$, r being the radius distance from the FS-laser beam centerline.

Moreover, the laser beam through the objective lens forms the surface damage threshold of sapphire. In this study, the threshold fluence indicates that a Gaussian beam of the FS laser can be determined by measuring the diameter of the ablated area and the pulse energy. The threshold fluence corresponds to the minimum energy per unit surface required to induce an ablation change of the sapphire surface. The laser energy is an experimental parameter whose value can be easily measured by a power meter. To achieve the patterned structures, the peak fluence of the FS-laser spot must be precisely controlled above the threshold fluence of sapphire [24]. Thus, the threshold fluence can be defined as a function of effective pulse energy for structure patterning and a critical parameter on the material surface of the component in the laser process. Under well-controlled conditions, a microstructure with a 5-μm round hole on the sapphire substrate can be easily formed at the energy fluence of 55.7 J/cm^2 because the FS-laser beam has a radius of the $1/e^2$ beam. In addition, Fig. 2b indicates that the FS-laser beam is of a Gaussian distribution, and does not form cracks around the ablated craters. Furthermore, the parameters of a Gaussian pulse profile are shown schematically in Fig. 2c from the calculated Eqs. (1) and (2).

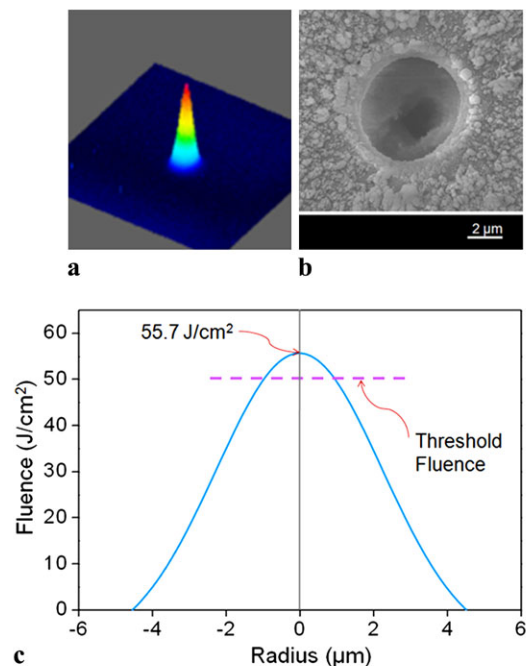

Fig. 2 Measured results of (**a**) FS-laser intensity distribution and (**b**) an example of a 5-μm round hole on the surface of sapphire substrate machined using a FS-laser process. (**c**) Calculated Gaussian energy fluence of FS-laser pulse. The energy fluence of the FS laser must exceed F_{th} for sapphire material to be removed

3.1 Damage threshold in a FS-laser process

In a FS-laser process, the damage threshold of sapphire samples with the current experimental setup should be determined first. To effectively fabricate the microstructures on

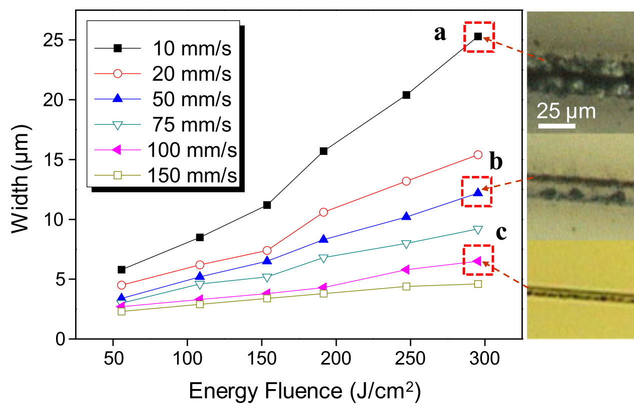

Fig. 3 Variations in line width of sapphire substrate microstructures as function of energy fluence and scanning speed. The *right-hand insets* show OM images of the laser-processed line showing processing quality of sapphire substrate microstructures at scanning speed of (**a**) 10 mm/s, (**b**) 50 mm/s and (**c**) 100 mm/s under an energy fluence of 295.3 J/cm^2

the sapphire surface, it is essential to investigate the energy fluence dependence of the line width on scanning speed. The relationship between the line width and the energy fluence is investigated with the change of scanning speed. Figure 3 shows the ablation line widths measured at different energy fluences. It can be seen that line width enlarges with increase in energy fluence. As just mentioned with respect to Fig. 2c, the ablation threshold of energy fluence can be effectively controlled at 50 J/cm^2; that is, the laser pulse energy is ∼3 μJ. Moreover, when using a low scanning speed of 10 mm/s, the accumulation of damage by laser ablation with multiple pulses generates ablation craters and increases the line width at energy fluences exceeding 200 J/cm^2, as marked in (a)–(c) in Fig. 3. Therefore, adopting a high energy fluence is disadvantageous for fabricating a short line width, as shown in Fig. 3, right-hand insets. To further investigate the quality of fabricated line structures, Fig. 4 displays the ablation line widths measured by SEM images at different scanning speeds. At a low energy fluence and a low scanning speed, an ablation structure without craters can be fabricated. However, a FS-pulse laser beam generates ablation craters at a high energy fluence and a low scanning speed. In summary, adopting a low energy fluence helps prevent damage of the fabricated microstructures on the sapphire surface.

It must be noted that the sapphire usually has no absorption at 517 nm (the frequency doubling of the Yb FS-laser wavelength). Since the sapphire surface is irradiated by the FS laser with no absorption wavelength, the linear absorption of the laser radiation does not occur. However, the energy of the Yb FS laser can offer a sufficiently high peak fluence within very short pulse durations. The very short time scale of FS-laser pulses increases the probability of multiple-photon absorption, that is, a nonlinear process [25, 26]. Though the typical energy band gap for sapphire is above 8 eV, an electron of the FS laser can simultaneously absorb the energy from multiple photons to exceed the band-gap occurrence leading to the sapphire ionization, which is proposed as a main mechanism of the sapphire surface patterning by a much lower energy laser. Though the doubled frequency of the FS-laser wavelength is used, the energy conversion efficiency from FS-laser pulses can exceed 60 % as evidenced in previous works for many dielectric materials [21, 27, 28].

Sapphire has a characteristic of high hardness; thus, obtaining suitable parameters of the FS-laser process is necessary for fabricating well-shaped microsize structures, such as gratings and square arrays. The Yb FS-laser patterning is predominately a nonlinear process to the sapphire ablation occurring within the focal region, which can be controlled by adjusting the pulse energy within the focal spot (ablation threshold). The energy efficiency of the FS laser can be considered as the energy fluence control. Based on the accurate energy fluence control, the FS-laser energy is much less than the band gap of sapphire for forming a crater on a laser-irradiated surface. Hence, this study chooses an appropriate scanning speed and an energy fluence to fabricate the sapphire microstructures with the least HAZ effect. To optimize the gratings and square arrays on the sapphire surfaces, the scanning speed and energy fluence of a FS-laser process are set constant at 50 mm/s and 95.34 J/cm^2, respectively.

3.2 1-D and 2-D fabricating microstructures

In this study, four types can be obtained with different geometric sizes as in Fig. 5a–d, in which the results are in Fig. 6a–d, respectively. As mentioned above, the optimum scanning speed (50 mm/s) and energy fluence (95.34 J/cm^2) of the FS-laser process can be used here. Figure 6a shows sapphire of one-dimensional (1-D) grating microstructures including a width of 5.6 μm with a period of 10 μm. The center portion of the groove is deeper owing to the high energy fluence of the laser in the center of the beam. Though there are serrations on the edges of the grating structures, it can be seen that the FS-laser system provides a potential process for forming fine microstructures. With the same scanning speed and energy fluence used for patterning one-dimensional grating microstructures, the sapphire microstructure of a two-dimensional (2-D) square array with a width of 11.8 μm and a period of 20 μm can be fabricated by a FS-laser process, as shown in Fig. 6b. To further study the characteristics of the fabricated microstructures by the FS-laser process, in this paper we patterned inclined groove-shaped microarray structures. Sapphire of inclined groove-based microarray structures with the same sideward angles is presented in Fig. 6c, and a two-dimensional square array is fabricated with a width

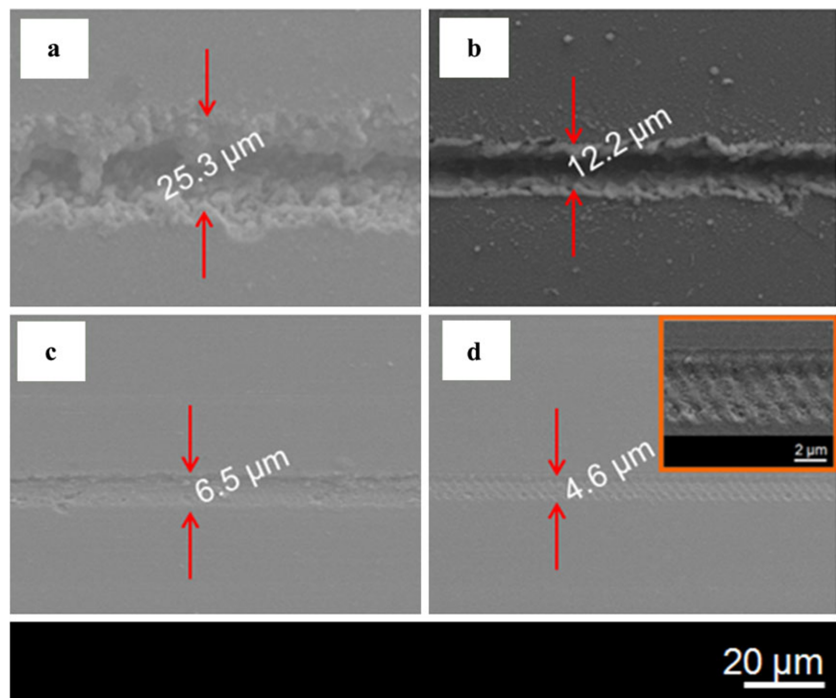

Fig. 4 SEM images of the laser-processed line showing processing quality of sapphire substrate microstructures at scanning speed of (**a**) 10 mm/s, (**b**) 50 mm/s, (**c**) 100 mm/s and (**d**) 150 mm/s under an energy fluence of 295.3 J/cm^2. The *inset* of (**d**) shows a magnified view of the pattern

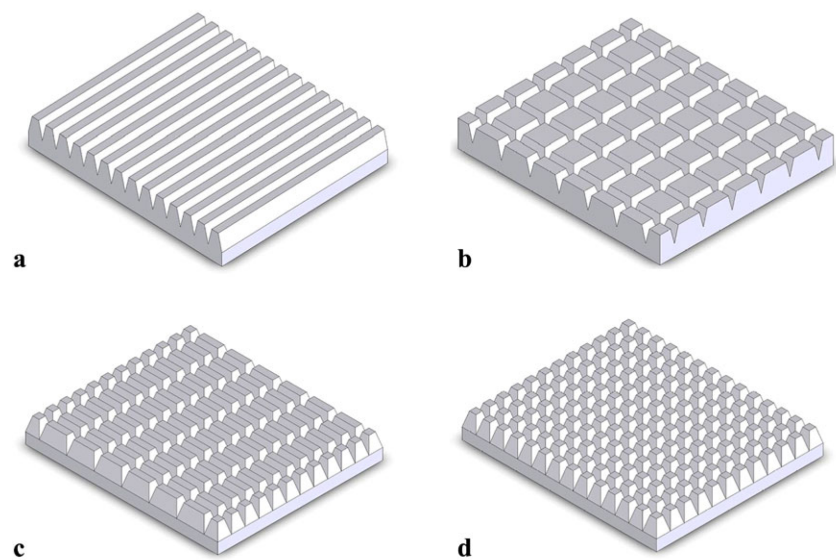

Fig. 5 Schematic of FS-laser-fabricated microstructures on the sapphire substrate. Different-size patterns: (**a**) gratings (width: 5.6 μm; period: 10 μm), (**b**) square array (width: 11.8 μm; period: 20 μm), (**c**) inclined groove-based array (period: 20 μm) and (**d**) square array (width: 8.1 μm; period: 10 μm)

of 8.1 μm and a period of 10 μm, as shown in Fig. 6d. Although the FS laser is capable of micromachining the square array structures on the sapphire surface, there are still some brittle and zigzag shapes on the sapphire substrate surface, which may result from the strong energy fluence of the laser for generating these shapes. These phenomena are similar to the findings obtained by Semaltianos et al. [29].

Additionally, it can be found that the small-dimension patterns in Fig. 6d have many defects. FS-laser mask-less processing of the sapphire surface can be proposed for improving light-emitting diode (LED) performance and further micro-optical applications. Due to the defects on the sapphire surface, these surface-textured structures can be achieved by the high light-extraction efficiency. Besides, the minimum usable size for a two-dimensional square array using the FS laser can be achieved with 8.1-μm line width. However, the minimum usable size using the FS laser can be controlled. An example is shown in Fig. 3; the minimum usable size for patterning the structure can be achieved with 2.2-μm line width. Thus, except for the problem of the diffraction-limited beam, the practical feature size is controlled and determined by the energy fluence and scanning speed of the FS-laser process.

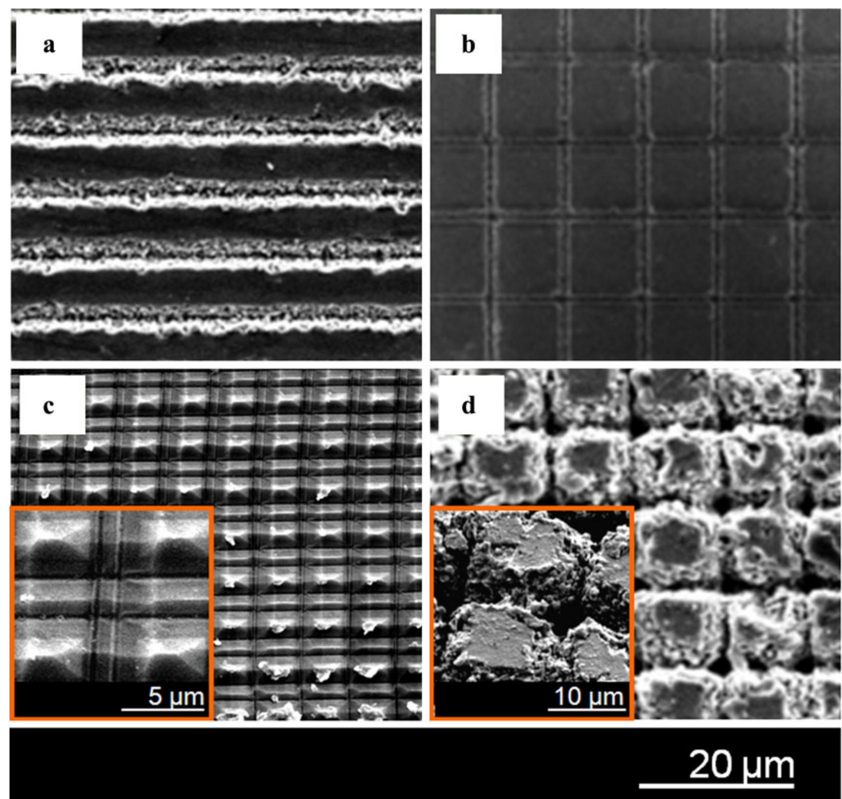

Fig. 6 SEM images of FS-laser-fabricated microstructures on the sapphire substrate. Different-size patterns: (**a**) gratings (width: 5.6 μm; period: 10 μm), (**b**) square array (width: 11.8 μm; period: 20 μm), (**c**) inclined groove-based array (period: 20 μm) and (**d**) square array (width: 8.1 μm; period: 10 μm). The *insets* of (**c**) and (**d**) shows magnified views of the pattern structures

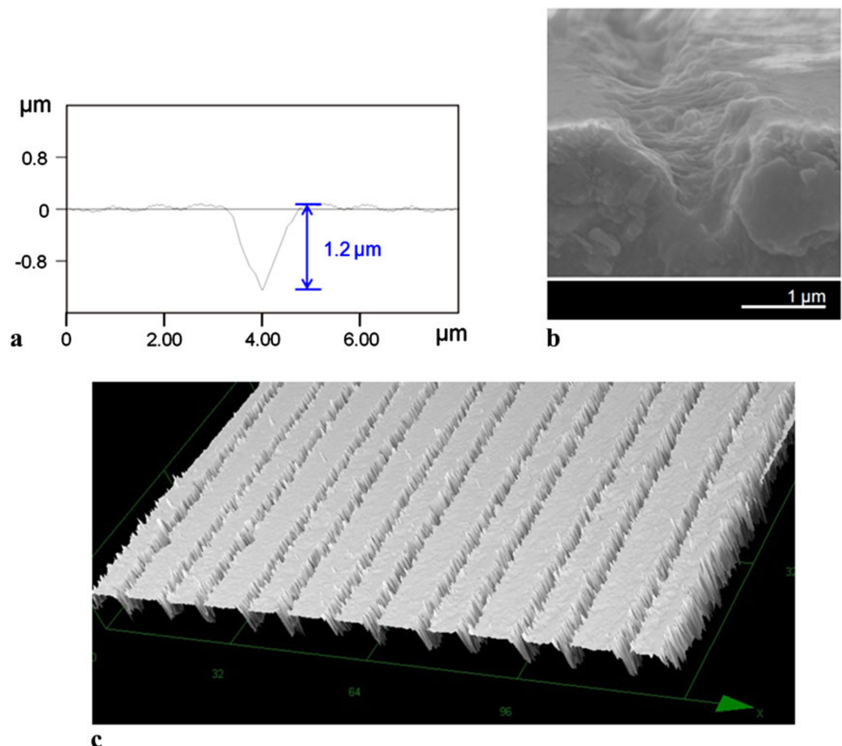

Fig. 7 Measured results of cross-sectional profile: (**a**) α-step measurement, (**b**) SEM image and (**c**) confocal microscope image. The depth of surface morphology on the sapphire surface is 1.2 ± 0.1 μm

The cross-sectional profile of the patterned sapphire microstructures is measured by the α-step (Fig. 7a). The constant scanning speed of 50 mm/s and the constant energy fluence of 95.34 J/cm^2 generate square array structures on the sapphire surface of 1.2 ± 0.1 μm depth. In addition, the surface morphology of the sapphire microstructures is exam-

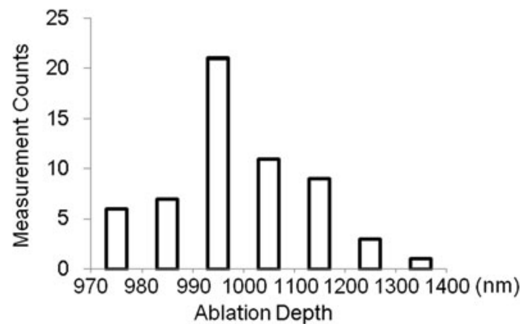

Fig. 8 Measurement counts of the depth of surface morphology on the sapphire surface

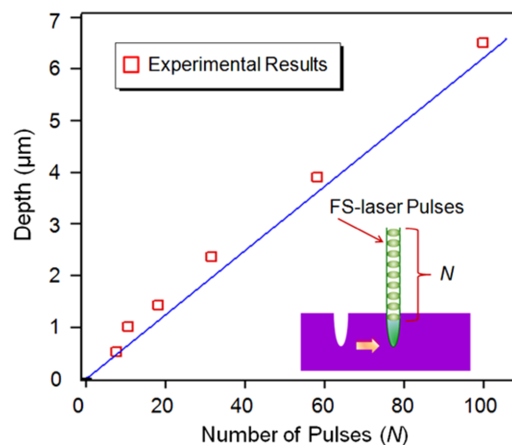

Fig. 9 Experimental results of ablation depth with increase in number of laser pulses on the sapphire substrate by a FS-laser process

ined in Fig. 7b. The previous section mentioned that the FS-laser intensity distribution is a Gaussian spatial beam profile; the SEM images (Fig. 7b) also display that the shape of removed sapphire is close to a Gaussian beam profile. Due to the hardness and brittleness of the sapphire substrate, it is difficult to carry out its cross-sectional measurement. The profile of the patterned sapphire surface is further measured by using a three-dimensional laser confocal microscope (LEXT OLS4000; Olympus Inc.) in Fig. 7c. It also shows that the sapphire surface has very few shoulders around the ablated lines. In other words, there is scarcely a bulge on the scanning edge, revealing that heat accumulation during laser fabrication does not result in heat-affected areas. Observing the surface morphology of the sapphire microstructures by the α-step measurement, it is shown in Fig. 8 that the surface roughness of the sapphire microstructures is only about 17 nm. By roughness in our study, we mean the root-mean-square (rms) deviation with three-sigma of the profile shape, which is the standard way to define roughness [30, 31].

Nevertheless, the precise control of the critical dimension of photoresist structures in the lithography process is more important when the dimensions of electronic devices are reduced to microscale or nanoscale regions [32–34]. Most of these works focused more on improving line-edge roughness than on improving surface roughness. In this study, the FS-laser process proposed for LED performances as mentioned above is used to pattern the sapphire material for the purpose of enhancing the light-extraction efficiency. Thus, the importance of the FS-laser process in improving the light-extraction efficiency of LEDs cannot be overemphasized; this is, sapphire patterned by the FS-laser process could enhance LEDs due to increasing of the light-escape probability. By that means, it is absolutely essential to measure the line-edge roughness of sapphire utilizing the FS-laser process. Moreover, the measurement of the line edge usually used a complex algorithm from a top-down SEM image of the process structures that is capable of another issue. Therefore, this study investigates the surface roughness only and here a required-structure microarray can be fabricated by a one-step FS-laser process.

3.3 Ablation depth

This study further analyzes the effect of the FS laser on ablation depth. During laser ablation with multiple pulses, the total number of pulses landing at a spot affects greatly the cutting size of the sapphire substrate. To investigate the relationship between the measured depth and the total number of laser pulses, this study uses the correlation parameter N given in Refs. [22, 23]:

$$N = \frac{Df}{V}, \tag{3}$$

where f is the repetition rate, D is the spot size and V is the scanning speed. That is, the total number of pulses at the surface structuring of sapphire is directly proportional to the spot size and to the ratio of the repetition rate to the scanning speed. The relationship between the measured depth and the total number of laser pulses is plotted in Fig. 9. For example, at the scanning speed of 50 mm/s and the energy fluence of 95.34 $\mathrm{J/cm^2}$, applying laser pulses with a correlation parameter of $N = 6$ perforates the sapphire substrate with the depth of 1 μm. A linear relation between the measured depth and the total number of laser pulses is found; that is, the ablation depth of sapphire is proportional to the number of laser pulses. Thus, changing the total number of pulses enables us to control the ablation depth and to design the layout of sapphire textured arrays.

4 Conclusions

The surface structuring of sapphire can be performed using an Yb FS-laser process, which has characteristics of being direct and easy. To determine the suitable energy fluence

and scanning speed of the FS-laser system, this study discusses the relationship between ablation line widths, energy fluences and scanning speeds. The OM images reveal that adopting a low energy fluence contributes to fabricating microstructures without generating craters on the sapphire surface. Under the FS-laser parameters of the energy fluence of 95.34 J/cm^2 and scanning speed of 50 mm/s, sapphire with a two-dimensional square array with the width of 8.1 µm, period of 10 µm and depth of 1.2 µm can be successfully achieved. The effect of the FS laser on the ablation depth is discussed. The measured depths and the total number of laser pulses are linearly dependent. Therefore, the FS-laser process can be effective and direct in fabricating order-based surface structures of sapphire, and can provide a potential process for light extraction and micro-optical applications.

Acknowledgements This work was funded by the National Science Council (NSC) of Taiwan, Republic of China under grant NSC 100-2218-E-003-001-MY2. We deeply appreciate Dr. Hung-Yi Lin, Dr. Min-Chieh Chou, Dr. Han-Ping Yang and Mr. Wen-Lang Lai from the Mechanical and Systems Research Laboratories at the Industrial Technology Research Institute for their advice and discussion on laser studies.

References

1. E.J. Höng, K.J. Byeon, H. Park, J. Hwang, H. Lee, K. Choi, G.Y. Jung, Mater. Sci. Eng. B, Adv. Funct. Solid-State Mater. **163**, 170 (2009)
2. D. Bruneel, G. Matras, R.L. Harzic, N. Huot, K. Konig, E. Audouard, Opt. Lasers Eng. **48**, 268 (2010)
3. J.S. Yahng, J.R. Nam, S.C. Jeoung, Opt. Lasers Eng. **47**, 815 (2009)
4. A. Dalili, B. Tan, K. Venkatakrishnan, Opt. Lasers Eng. **48**, 346 (2010)
5. X.Y. Tan, D.M. Zhang, M. Feng, Z.H. Li, D. Yi, X.Z. Zhang, Trans. Nonferr. Met. Soc. China **19**, 1645 (2009)
6. H. Jha, T. Kikuchi, M. Sakairi, H. Takahashi, Electrochim. Acta **52**, 4724 (2007)
7. M.S. Ahsan, F. Ahmed, Y.G. Kim, M.S. Lee, B.G.J. Martin, Appl. Surf. Sci. **257**, 7771 (2011)
8. A.Y. Vorobyev, C. Guo, Appl. Phys. A **86**, 235 (2007)
9. R.L. Harzic, D. Dörr, D. Sauer, M. Neumeier, M. Epple, H. Zimmermann, F. Stracke, Phys. Procedia **12**, 29 (2011)
10. S.M. Eaton, M.L. Ng, R. Osellame, P.R. Herman, J. Non-Cryst. Solids **357**, 2387 (2011)
11. S. Matsuo, K. Tokumi, T. Tomita, S. Hashimoto, Laser Chem. **2008**, 892721 (2008)
12. L. Qi, K. Nishii, M. Yasui, H. Aoki, Y. Namba, in *Proc. ASPE* (2009), p. 231
13. M. Shinoda, R. Gattass, E. Mazur, J. Appl. Phys. **105**, 053102 (2009)
14. S. Noel, J. Hermann, T. Itina, Appl. Surf. Sci. **253**, 6310 (2007)
15. G. Matras, N. Huot, E. Baubeau, E. Audouard, Opt. Express **15**, 7528 (2007)
16. B. Rethfeld, K. Sokolowski-Tinten, D. von der Linde, S.I. Anisimov, Appl. Phys. A **79**, 571 (2002)
17. S.I. Anisimov, B.L. Kapeliovich, T.L. Perel'man, Sov. Phys. JETP **39**, 375 (1974)
18. T. Gertus, M. Mikutis, V. Smilgevicius, Phys. Procedia **12**, 94 (2011)
19. C.A. Aguilar, Y. Lu, S. Mao, S. Chen, Biomaterials **26**, 7642 (2005)
20. C.J. Hayden, C. Dalton, Appl. Surf. Sci. **256**, 3761 (2010)
21. M. Wiesner, J. Ihlemann, Phys. Procedia **12**, 239 (2011)
22. G. Pal, A. Dutta, K. Mitra, M.S. Grace, A. Amat, T.B. Romanczyk, X.J. Wu, K. Chakrabarti, J. Anders, E. Gorman, R.W. Waynant, D.B. Tata, J. Photochem. Photobiol. B, Biol. **86**, 252 (2007)
23. H. Huang, Z. Guo, J. Micromech. Microeng. **19**, 055007 (2009)
24. K. Venkatakrishnan, B. Tan, N.R. Sivakumar, Opt. Laser Technol. **34**, 575 (2002)
25. A. Heltzel, A. Battula, J.R. Howell, S. Chen, J. Heat Transf. **129**(1), 53 (2007)
26. A.-C. Tien, S. Backus, H. Kapteyn, M. Murnane, G. Mourou, Phys. Rev. Lett. **82**(19), 3883 (1999)
27. P. Sprangle, J.R. Peñano, B. Hafizi, C.A. Kapetanakos, Phys. Rev. E **69**, 066415 (2004)
28. S.-N. Luo, P.D. Peralta, C. Ma, D.L. Paisley, S.R. Greenfield, E.N. Loomis, Appl. Surf. Sci. **253**(24), 9457 (2007)
29. N.G. Semaltianos, C. Koidis, C. Pitsalidis, P. Karagiannidis, S. Logothetidis, W. Perrie, D. Liu, S.P. Edwardson, E. Fearon, R.J. Potter, G. Dearden, K.G. Watkins, Synth. Met. **161**, 431 (2011)
30. J.M. Howell, Ann. Math. Stat. **20**, 305 (1949)
31. K. Selinidis, E. Thompson, G. Schmid, N. Stacey, J. Perez, J. Maltabes, S.V. Sreenivasan, D.J. Resnick, A. Fujii, Y. Sakai, S. Sasaki, N. Hayashi, J. Vac. Sci. Technol. B **26**(6), 2410 (2008)
32. S. Kaya, A.R. Brown, A. Asenov, D. Magot, T. Linton, in *Proc. SISPAD* (2001), p. 78
33. S. Xiong, J. Bokor, Q. Xiang, P. Fishe, I. Dudley, P. Rao, Proc. SPIE **4689**, 733 (2003)
34. B. Bilski, K. Frenner, W. Osten, Opt. Express **19**, 19967 (2011)